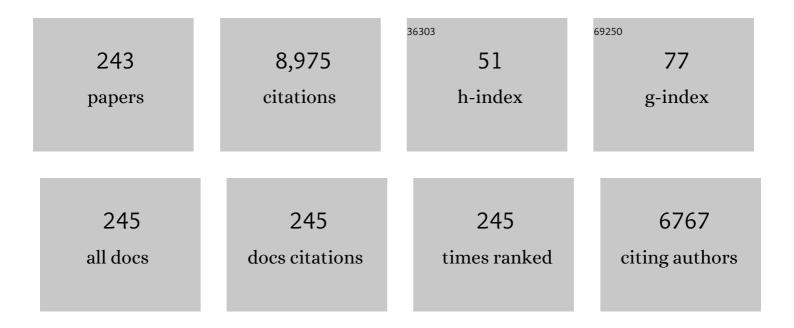
Xiandeng Hou Hou

List of Publications by Year in descending order

Source: https://exaly.com/author-pdf/8372338/publications.pdf Version: 2024-02-01



#	Article	IF	CITATIONS
1	Electrochemically Generated versus Photoexcited Luminescence from Semiconductor Nanomaterials: Bridging the Valley between Two Worlds. Chemical Reviews, 2014, 114, 11027-11059.	47.7	265
2	Semicondutor quantum dots-based metal ion probes. Nanoscale, 2014, 6, 43-64.	5.6	264
3	Phosphorescent Carbon Dots for Highly Efficient Oxygen Photosensitization and as Photo-oxidative Nanozymes. ACS Applied Materials & Interfaces, 2018, 10, 40808-40814.	8.0	192
4	Photo-induced chemical vapor generation with formic acid for ultrasensitive atomic fluorescence spectrometric determination of mercury: potential application to mercury speciation in water. Journal of Analytical Atomic Spectrometry, 2005, 20, 746.	3.0	185
5	Applications of chemical vapor generation in non-tetrahydroborate media to analytical atomic spectrometry. Journal of Analytical Atomic Spectrometry, 2010, 25, 1217.	3.0	156
6	Optically-active nanocrystals for inner filter effect-based fluorescence sensing: Achieving better spectral overlap. TrAC - Trends in Analytical Chemistry, 2019, 110, 183-190.	11.4	155
7	Critical evaluation of the application of photochemical vapor generation in analytical atomic spectrometry. Analytical and Bioanalytical Chemistry, 2007, 388, 769-774.	3.7	136
8	Ultrarapid in Situ Synthesis of Cu ₂ S Nanosheet Arrays on Copper Foam with Room-Temperature-Active lodine Plasma for Efficient and Cost-Effective Oxygen Evolution. ACS Catalysis, 2018, 8, 3859-3864.	11.2	129
9	Microwave-induced fast incorporation of titanium into UiO-66 metal–organic frameworks for enhanced photocatalytic properties. Chemical Communications, 2017, 53, 3361-3364.	4.1	121
10	Fe ₃ Nâ€Co ₂ N Nanowires Array: A Nonâ€Nobleâ€Metal Bifunctional Catalyst Electrode for Highâ€Performance Glucose Oxidation and H ₂ O ₂ Reduction toward Nonâ€Enzymatic Sensing Applications. Chemistry - A European Journal, 2017, 23, 5214-5218.	3.3	117
11	Titanium Incorporation into Zrâ€Porphyrinic Metal–Organic Frameworks with Enhanced Antibacterial Activity against Multidrugâ€Resistant Pathogens. Small, 2020, 16, e1906240.	10.0	116
12	Visual Detection of Fluoride Anions Using Mixed Lanthanide Metal–Organic Frameworks with a Smartphone. Analytical Chemistry, 2020, 92, 2097-2102.	6.5	115
13	A Target-Triggered DNAzyme Motor Enabling Homogeneous, Amplified Detection of Proteins. Analytical Chemistry, 2017, 89, 12888-12895.	6.5	114
14	Recent Advances in Portable Xâ€Ray Fluorescence Spectrometry. Applied Spectroscopy Reviews, 2004, 39, 1-25.	6.7	112
15	Determination of Cadmium in Biological Samples. Applied Spectroscopy Reviews, 2006, 41, 35-75.	6.7	111
16	Recent Advance of Hydride Generation–Analytical Atomic Spectrometry: Part I—Technique Development. Applied Spectroscopy Reviews, 2012, 47, 382-413.	6.7	97
17	Temperature and nano-TiO2 controlled photochemical vapor generation for inorganic selenium speciation analysis by AFS or ICP-MS without chromatographic separation. Journal of Analytical Atomic Spectrometry, 2008, 23, 514.	3.0	94
18	UV photochemical vapor generation–atomic fluorescence spectrometric determination of conventional hydride generation elements. Microchemical Journal, 2010, 95, 32-37.	4.5	94

#	Article	IF	CITATIONS
19	Proteinâ€Directed Synthesis of Mnâ€Doped ZnS Quantum Dots: A Dualâ€Channel Biosensor for Two Proteins. Chemistry - A European Journal, 2013, 19, 7473-7479.	3.3	90
20	UV Photochemical Vapor Generation Sample Introduction for Determination of Ni, Fe, and Se in Biological Tissue by Isotope Dilution ICPMS. Analytical Chemistry, 2010, 82, 3899-3904.	6.5	89
21	Porous chitosan/hydroxyapatite composite membrane for dyes static and dynamic removal from aqueous solution. Journal of Hazardous Materials, 2017, 338, 241-249.	12.4	88
22	Electrothermal Vaporization for Universal Liquid Sample Introduction to Dielectric Barrier Discharge Microplasma for Portable Atomic Emission Spectrometry. Analytical Chemistry, 2014, 86, 5220-5224.	6.5	83
23	Versatile Thin-Film Reactor for Photochemical Vapor Generation. Analytical Chemistry, 2010, 82, 3086-3093.	6.5	78
24	High-Yield UV-Photochemical Vapor Generation of Iron for Sample Introduction with Inductively Coupled Plasma Optical Emission Spectrometry. Analytical Chemistry, 2010, 82, 2996-3001.	6.5	77
25	Sample matrix-assisted photo-induced chemical vapor generation: a reagent free green analytical method for ultrasensitive detection of mercury in wine or liquor samples. Journal of Analytical Atomic Spectrometry, 2006, 21, 82-85.	3.0	74
26	Recent Advance of Hydride Generation–Analytical Atomic Spectrometry: Part II—Analysis of Real Samples. Applied Spectroscopy Reviews, 2012, 47, 495-517.	6.7	74
27	Ultrasensitive Speciation Analysis of Mercury in Rice by Headspace Solid Phase Microextraction Using Porous Carbons and Gas Chromatography-Dielectric Barrier Discharge Optical Emission Spectrometry. Environmental Science & Technology, 2016, 50, 2468-2476.	10.0	72
28	Copper Ion Assisted Photochemical Vapor Generation of Chlorine for Its Sensitive Determination by Sector Field Inductively Coupled Plasma Mass Spectrometry. Analytical Chemistry, 2018, 90, 4112-4118.	6.5	72
29	Recent trends in atomic fluorescence spectrometry towards miniaturized instrumentation-A review. Analytica Chimica Acta, 2018, 1019, 25-37.	5.4	72
30	Cerium-based UiO-66 metal–organic frameworks explored as efficient redox catalysts: titanium incorporation and generation of abundant oxygen vacancies. Chemical Communications, 2019, 55, 13959-13962.	4.1	72
31	Spectroscopy: The Best Way Toward Green Analytical Chemistry?. Applied Spectroscopy Reviews, 2007, 42, 119-138.	6.7	71
32	Determination of Hg, Fe, Ni, and Co by Miniaturized Optical Emission Spectrometry Integrated with Flow Injection Photochemical Vapor Generation and Point Discharge. Analytical Chemistry, 2015, 87, 10712-10718.	6.5	71
33	Vapor generation in dielectric barrier discharge for sensitive detection of mercury by inductively coupled plasma optical emission spectrometry. Journal of Analytical Atomic Spectrometry, 2011, 26, 1204.	3.0	70
34	Hydride Generation for Headspace Solid-Phase Extraction with CdTe Quantum Dots Immobilized on Paper for Sensitive Visual Detection of Selenium. Analytical Chemistry, 2016, 88, 789-795.	6.5	70
35	Headspace Solid-Phase Microextraction Coupled to Miniaturized Microplasma Optical Emission Spectrometry for Detection of Mercury and Lead. Analytical Chemistry, 2018, 90, 3683-3691.	6.5	69
36	Tungsten devices in analytical atomic spectrometry. Spectrochimica Acta, Part B: Atomic Spectroscopy, 2002, 57, 659-688.	2.9	67

#	Article	IF	CITATIONS
37	Longâ€Lived Charge Carriers in Mnâ€Doped CdS Quantum Dots for Photoelectrochemical Cytosensing. Chemistry - A European Journal, 2015, 21, 5129-5135.	3.3	67
38	Dielectric Barrier Discharge in Analytical Spectrometry. Applied Spectroscopy Reviews, 2011, 46, 368-387.	6.7	66
39	UV photochemical vapor generation and in situ preconcentration for determination of ultra-trace nickel by flow injection graphite furnace atomic absorption spectrometry. Journal of Analytical Atomic Spectrometry, 2009, 24, 1452.	3.0	65
40	Low-toxic Mn-doped ZnSe@ZnS quantum dots conjugated with nano-hydroxyapatite for cell imaging. Nanoscale, 2014, 6, 14319-14325.	5.6	63
41	Room Temperature Cation Exchange Reaction in Nanocrystals for Ultrasensitive Speciation Analysis of Silver Ions and Silver Nanoparticles. Analytical Chemistry, 2015, 87, 6584-6591.	6.5	63
42	Phosphorescent Differential Sensing of Physiological Phosphates with Lanthanide Ions-Modified Mn-Doped ZnCdS Quantum Dots. Analytical Chemistry, 2016, 88, 5892-5897.	6.5	60
43	Dielectric Barrier Discharge Carbon Atomic Emission Spectrometer: Universal GC Detector for Volatile Carbon-Containing Compounds. Analytical Chemistry, 2014, 86, 936-942.	6.5	58
44	Modulation of the Singlet Oxygen Generation from the Double Strand DNA-SYBR Green I Complex Mediated by T-Melamine-T Mismatch for Visual Detection of Melamine. Analytical Chemistry, 2017, 89, 5101-5106.	6.5	58
45	Low Power, Low Temperature and Atmospheric Pressure Plasmaâ€Induced Polymerization: Facile Synthesis and Crystal Regulation of Covalent Organic Frameworks. Angewandte Chemie - International Edition, 2021, 60, 9984-9989.	13.8	57
46	On-line preconcentration and in situ photochemical vapor generation in coiled reactor for speciation analysis of mercury and methylmercury by atomic fluorescence spectrometry. Journal of Analytical Atomic Spectrometry, 2011, 26, 126-132.	3.0	56
47	Single Drop Solution Electrode Glow Discharge for Plasma Assisted-Chemical Vapor Generation: Sensitive Detection of Zinc and Cadmium in Limited Amounts of Samples. Analytical Chemistry, 2014, 86, 12093-12099.	6.5	56
48	Gold Nanoparticle-Based Colorimetric Assay for Selenium Detection via Hydride Generation. Analytical Chemistry, 2017, 89, 4695-4700.	6.5	56
49	AuNPs/COFs as a new type of SERS substrate for sensitive recognition of polyaromatic hydrocarbons. Chemical Communications, 2017, 53, 11044-11047.	4.1	55
50	Nanomaterials for photochemical vapor generation-analytical atomic spectrometry. TrAC - Trends in Analytical Chemistry, 2019, 114, 242-250.	11.4	55
51	Dielectric Barrier Discharge Molecular Emission Spectrometer as Multichannel GC Detector for Halohydrocarbons. Analytical Chemistry, 2011, 83, 5050-5055.	6.5	54
52	Exploring the tunable excitation of QDs to maximize the overlap with the absorber for inner filter effect-based phosphorescence sensing of alkaline phosphatase. Nanoscale, 2017, 9, 15606-15611.	5.6	52
53	Analyte-Activable Probe for Protease Based on Cytochrome C-Capped Mn: ZnS Quantum Dots. Analytical Chemistry, 2014, 86, 10078-10083.	6.5	51
54	Miniaturized Dielectric Barrier Discharge Carbon Atomic Emission Spectrometry with Online Microwave-Assisted Oxidation for Determination of Total Organic Carbon. Analytical Chemistry, 2014, 86, 6214-6219.	6.5	51

#	Article	IF	CITATIONS
55	Nanomaterials in speciation analysis of mercury, arsenic, selenium, and chromium by analytical atomic/molecular spectrometry. Applied Spectroscopy Reviews, 2018, 53, 333-348.	6.7	51
56	Photocatalytic oxidation of TMB with the double stranded DNA–SYBR Green I complex for label-free and universal colorimetric bioassay. Chemical Communications, 2015, 51, 14465-14468.	4.1	50
57	Dielectric barrier discharge-assisted one-pot synthesis of carbon quantum dots as fluorescent probes for selective and sensitive detection of hydrogen peroxide and glucose. Talanta, 2015, 142, 51-56.	5.5	49
58	Colorimetric sensing of bithiols using photocatalytic UiO-66(NH2) as H2O2-free peroxidase mimics. Talanta, 2016, 158, 276-282.	5.5	49
59	<i>In situ</i> formation of nano-CdSe as a photocatalyst: cadmium ion-enhanced photochemical vapour generation directly from Se(<scp>vi</scp>). Chemical Communications, 2018, 54, 4874-4877.	4.1	49
60	Disposable Paper-Based Analytical Device for Visual Speciation Analysis of Ag(I) and Silver Nanoparticles (AgNPs). Analytical Chemistry, 2019, 91, 3359-3366.	6.5	49
61	Cobalt and Copper Ions Synergistically Enhanced Photochemical Vapor Generation of Molybdenum: Mechanism Study and Analysis of Water Samples. Analytical Chemistry, 2019, 91, 5938-5944.	6.5	49
62	Tungsten Coil Devices in Atomic Spectrometry: Absorption, Fluorescence, and Emission. Analytical Sciences, 2001, 17, 175-180.	1.6	48
63	Evaluation of tungsten coil electrothermal vaporization-Ar/H2 flame atomic fluorescence spectrometry for determination of eight traditional hydride-forming elements and cadmium without chemical vapor generation. Talanta, 2008, 74, 505-511.	5.5	48
64	Direct Determination of Trace Antimony in Natural Waters by Photochemical Vapor Generation ICPMS: Method Optimization and Comparison of Quantitation Strategies. Analytical Chemistry, 2015, 87, 7996-8004.	6.5	47
65	Point Discharge Optical Emission Spectrometer as a Gas Chromatography (GC) Detector for Speciation Analysis of Mercury in Human Hair. Analytical Chemistry, 2018, 90, 11996-12003.	6.5	47
66	Recyclable Decoration of Amine-Functionalized Magnetic Nanoparticles with Ni ²⁺ for Determination of Histidine by Photochemical Vapor Generation Atomic Spectrometry. Analytical Chemistry, 2014, 86, 842-848.	6.5	46
67	Cost-effective and environmentally friendly synthesis of 3D Ni ₂ P from scrap nickel for highly efficient hydrogen evolution in both acidic and alkaline media. Journal of Materials Chemistry A, 2018, 6, 4088-4094.	10.3	46
68	Label-Free and Separation-Free Atomic Fluorescence Spectrometry-Based Bioassay: Sensitive Determination of Single-Strand DNA, Protein, and Double-Strand DNA. Analytical Chemistry, 2016, 88, 2065-2071.	6.5	45
69	Hydride generation-point discharge microplasma-optical emission spectrometry for the determination of trace As, Bi, Sb and Sn. Journal of Analytical Atomic Spectrometry, 2016, 31, 2427-2433.	3.0	44
70	Simultaneously Broadened Visible Light Absorption and Boosted Intersystem Crossing in Platinum-Doped Graphite Carbon Nitride for Enhanced Photosensitization. ACS Applied Materials & Interfaces, 2019, 11, 20770-20777.	8.0	44
71	Enhancement of photoredox catalytic properties of porphyrinic metal–organic frameworks based on titanium incorporation <i>via</i> post-synthetic modification. Chemical Communications, 2018, 54, 8610-8613.	4.1	43
72	Plasma-catalysed reaction M ⁿ⁺ + L–H → MOFs: facile and tunable construction of metal–organic frameworks in dielectric barrier discharge. Chemical Communications, 2019, 55, 12192-12195.	4.1	43

#	Article	IF	CITATIONS
73	Facile colorimetric sensing of Pb 2+ using bimetallic lanthanide metal-organic frameworks as luminescent probe for field screen analysis of lead-polluted environmental water. Microchemical Journal, 2017, 134, 140-145.	4.5	43
74	Photochemical vapor generation of carbonyl for ultrasensitive atomic fluorescence spectrometric determination of cobalt. Microchemical Journal, 2010, 96, 277-282.	4.5	42
75	Amine-functionalized titanium metal organic framework for photochemical vapor generation for determination of selenium by inductively coupled plasma optical emission spectrometry. Microchemical Journal, 2017, 132, 245-250.	4.5	41
76	Strand Displacement-Induced Enzyme-Free Amplification for Label-Free and Separation-Free Ultrasensitive Atomic Fluorescence Spectrometric Detection of Nucleic Acids and Proteins. Analytical Chemistry, 2016, 88, 12386-12392.	6.5	40
77	Selective reduction-based, highly sensitive and homogeneous detection of iodide and melamine using chemical vapour generation-atomic fluorescence spectrometry. Chemical Communications, 2018, 54, 4696-4699.	4.1	40
78	Atomic absorption spectrometric determination of trace tellurium after hydride trapping on platinum-coated tungsten coil. Microchemical Journal, 2010, 95, 320-325.	4.5	38
79	Single-Drop Solution Electrode Discharge-Induced Cold Vapor Generation Coupling to Matrix Solid-Phase Dispersion: A Robust Approach for Sensitive Quantification of Total Mercury Distribution in Fish. Analytical Chemistry, 2017, 89, 2093-2100.	6.5	38
80	Direct detection of mercury in vapor and aerosol from chemical atomization and nebulization at ambient temperature: exploiting the flame atomic absorption spectrometer. Journal of Analytical Atomic Spectrometry, 2005, 20, 760.	3.0	37
81	Arc/Spark Optical Emission Spectrometry: Principles, Instrumentation, and Recent Applications. Applied Spectroscopy Reviews, 2005, 40, 165-185.	6.7	37
82	Direct and simultaneous quantification of ATP, ADP and AMP by 1H and 31P Nuclear Magnetic Resonance spectroscopy. Talanta, 2016, 150, 485-492.	5.5	37
83	UV-induced carbonyl generation with formic acid for sensitive determination of nickel by atomic fluorescence spectrometry. Talanta, 2010, 80, 1239-1244.	5.5	36
84	Metal organic frameworks CAU-1 as new photocatalyst for photochemical vapour generation for analytical atomic spectrometry. Journal of Analytical Atomic Spectrometry, 2015, 30, 339-342.	3.0	36
85	Multivariate optimization of photochemical vapor generation for direct determination of arsenic in seawater by inductively coupled plasma mass spectrometry. Analytica Chimica Acta, 2015, 901, 34-40.	5.4	35
86	Plasma-assisted quadruple-channel optosensing of proteins and cells with Mn-doped ZnS quantum dots. Nanoscale, 2016, 8, 4291-4298.	5.6	35
87	Colorimetric determination of uranyl (<mml:math)="" etqq1<="" td="" tj="" xmlns:mml="http://www.w3.org/1998/Math/MathML"><td>1 0.7843 5.5</td><td>14 rgBT /Ov 35</td></mml:math>	1 0.7843 5.5	14 rgBT /Ov 35
88	Single Bimetallic Lanthanide-Based Metal–Organic Frameworks for Visual Decoding of a Broad Spectrum of Molecules. Analytical Chemistry, 2020, 92, 5500-5508.	6.5	35
89	Determination of Cadmium in Biological Samples: An Update from 2006 to 2011. Applied Spectroscopy Reviews, 2012, 47, 327-370.	6.7	34
90	Online solid sampling platform using multi-wall carbon nanotube assisted matrix solid phase dispersion for mercury speciation in fish by HPLC-ICP-MS. Journal of Analytical Atomic Spectrometry, 2015, 30, 882-887.	3.0	34

#	Article	IF	CITATIONS
91	Sensitive detection of bisphenol A by coupling solid phase microextraction based on monolayer graphene-coated Ag nanoparticles on Si fibers to surface enhanced Raman spectroscopy. Talanta, 2018, 187, 13-18.	5.5	34
92	Integration of Flow Injection Capillary Liquid Electrode Discharge Optical Emission Spectrometry and Microplasma-Induced Vapor Generation: A System for Detection of Ultratrace Hg and Cd in a Single Drop of Human Whole Blood. Analytical Chemistry, 2019, 91, 2701-2709.	6.5	34
93	DETERMINATION OF PLATINUM IN CLINICAL SAMPLES. Applied Spectroscopy Reviews, 2002, 37, 57-88.	6.7	33
94	Ultrasensitive determination of selenium by atomic fluorescence spectrometry using nano-TiO ₂ pre-concentration and in situhydride generation. Journal of Analytical Atomic Spectrometry, 2012, 27, 270-275.	3.0	33
95	Chemical Vapor Generation for Determination of Mercury by Inductively Coupled Plasma Mass Spectrometry. Applied Spectroscopy Reviews, 2007, 42, 79-102.	6.7	32
96	Thin film hydride generation: determination of ultra-trace copper by flow injection in situ hydride trapping graphite furnace AAS. Journal of Analytical Atomic Spectrometry, 2010, 25, 1159.	3.0	32
97	Antibody-biotemplated HgS nanoparticles: Extremely sensitive labels for atomic fluorescence spectrometric immunoassay. Analyst, The, 2012, 137, 1473.	3.5	32
98	Point Discharge Microplasma Optical Emission Spectrometer: Hollow Electrode for Efficient Volatile Hydride/Mercury Sample Introduction and 3D-Printing for Compact Instrumentation. Analytical Chemistry, 2019, 91, 7001-7006.	6.5	32
99	Determination of selenium by tungsten coil atomic absorption spectrometry using iridium as a permanent chemical modifier. Spectrochimica Acta, Part B: Atomic Spectroscopy, 2001, 56, 203-214.	2.9	31
100	Determination of Arsenic and Mercury in Chinese Medicinal Herbs by Atomic Fluorescence Spectrometry with Closedâ€Vessel Microwave Digestion. Spectroscopy Letters, 2004, 37, 263-274.	1.0	31
101	Analytical Atomic Spectrometry for Nuclear Forensics. Applied Spectroscopy Reviews, 2005, 40, 245-267.	6.7	31
102	Recent Progress in Chemiluminescence for Gas Analysis. Applied Spectroscopy Reviews, 2010, 45, 474-489.	6.7	31
103	Preconcentration and in-situ photoreduction of trace selenium using TiO2 nanoparticles, followed by its determination by slurry photochemical vapor generation atomic fluorescence spectrometry. Mikrochimica Acta, 2014, 181, 197-204.	5.0	31
104	Integration of hydride generation and photochemical vapor generation for multi-element analysis of traditional Chinese medicine by ICP-OES. Microchemical Journal, 2015, 123, 164-169.	4.5	31
105	Continuous and Inexpensive Monitoring of Nonpurgeable Organic Carbon by Coupling High-Efficiency Photo-oxidation Vapor Generation with Miniaturized Point-Discharge Optical Emission Spectrometry. Environmental Science & Technology, 2017, 51, 9109-9117.	10.0	31
106	Chemical vapor generation by reaction of cadmium with potassium tetrahydroborate and sodium iodate in acidic aqueous solution for atomic fluorescence spectrometric application. Journal of Analytical Atomic Spectrometry, 2004, 19, 1010.	3.0	30
107	Photochemical vapor generation and in situ preconcentration for determination of mercury by graphite furnace atomic absorption spectrometry. Analytical Methods, 2015, 7, 3015-3021.	2.7	30
108	Pump- and Valve-Free Flow Injection Capillary Liquid Electrode Discharge Optical Emission Spectrometry Coupled to a Droplet Array Platform. Analytical Chemistry, 2017, 89, 703-710.	6.5	30

#	Article	IF	CITATIONS
109	Nano g-C3N4/TiO2 composite: A highly efficient photocatalyst for selenium (VI) photochemical vapor generation for its ultrasensitive AFS determination. Microchemical Journal, 2017, 135, 158-162.	4.5	30
110	Optical sensing at the nanobiointerface of metal ion–optically-active nanocrystals. Nanoscale, 2018, 10, 5035-5046.	5.6	30
111	A RGB-Type Quantum Dot-based Sensor Array for Sensitive Visual Detection of Trace Formaldehyde in Air. Scientific Reports, 2016, 6, 36794.	3.3	29
112	Determination of Trace Metals in Drinking Water Using Solid-Phase Extraction Disks and X-ray Fluorescence Spectrometry. Applied Spectroscopy, 2003, 57, 338-342.	2.2	28
113	Simultaneous determination of trace cadmium and lead in single human hair by tungsten electrothermal vaporization-flame atomic fluorescence spectrometry. Microchemical Journal, 2014, 114, 182-186.	4.5	28
114	Selective determination of Cr(â¥) and non-chromatographic speciation analysis of inorganic chromium by chemical vapor generation-inductively coupled plasma mass spectrometry. Talanta, 2020, 218, 121128.	5.5	28
115	Dielectric barrier discharge plasma for nanomaterials: Fabrication, modification and analytical applications. TrAC - Trends in Analytical Chemistry, 2022, 156, 116715.	11.4	28
116	Determination of Trace Cadmium and Zinc in Corn Kernels and Related Soil Samples by Atomic Absorption and Chemical Vapor Generation Atomic Fluorescence After Microwaveâ€Assisted Digestion. Spectroscopy Letters, 2006, 39, 29-43.	1.0	27
117	Three-Dimensional Printed Dual-Mode Chemical Vapor Generation Point Discharge Optical Emission Spectrometer for Field Speciation Analyses of Mercury and Inorganic Selenium. Analytical Chemistry, 2021, 93, 14923-14928.	6.5	27
118	Covalent triazine framework-1: A novel oxidase and peroxidase mimic. Microchemical Journal, 2017, 135, 91-99.	4.5	26
119	Recombinase Polymerase Amplification Coupled with a Photosensitization Colorimetric Assay for Fast <i>Salmonella</i> spp. Testing. Analytical Chemistry, 2021, 93, 6559-6566.	6.5	26
120	UV-induced atomization of gaseous mercury hydrides for atomic fluorescence spectrometric detection of inorganic and organic mercury after high performance liquid chromatographic separation. Journal of Analytical Atomic Spectrometry, 2013, 28, 510.	3.0	25
121	Phosphorescent inner filter effect-based sensing of xanthine oxidase and its inhibitors with Mn-doped ZnS quantum dots. Nanoscale, 2018, 10, 8477-8482.	5.6	25
122	Cobalt ion-enhanced photochemical vapor generation in a mixed acid medium for sensitive detection of tellurium(<scp>iv</scp>) by atomic fluorescence spectrometry. Journal of Analytical Atomic Spectrometry, 2020, 35, 1405-1411.	3.0	25
123	A colorimetric assay for the determination of trace arsenic based on in-situ formation of AuNPs with synergistic effect of arsine and iodide. Analytica Chimica Acta, 2021, 1144, 61-67.	5.4	25
124	Improved hollow fiber supported liquid–liquid–liquid membrane microextraction for speciation of inorganic and organic mercury by capillary electrophoresis. Analytical Methods, 2013, 5, 1185.	2.7	24
125	Flow injection hydride generation for on-atomizer trapping: Highly sensitive determination of cadmium by tungsten coil atomic absorption spectrometry. Microchemical Journal, 2014, 112, 7-12.	4.5	24
126	Glucose oxidase-directed, instant synthesis of Mn-doped ZnS quantum dots in neutral media with retained enzymatic activity: mechanistic study and biosensing application. Journal of Materials Chemistry B, 2015, 3, 5942-5950.	5.8	24

#	Article	IF	CITATIONS
127	A chemiluminescence metalloimmunoassay for sensitive detection of alpha-fetoprotein in human serum using Fe-MIL-88B-NH ₂ as a label. Applied Spectroscopy Reviews, 2016, 51, 517-526.	6.7	24
128	On-line UV photochemical generation of volatile copper species and its analytical application. Microchemical Journal, 2016, 124, 344-349.	4.5	24
129	AuNCs-Catalyzed Hydrogen Selenide Oxidation: Mechanism and Application for Headspace Fluorescent Detection of Se(IV). Analytical Chemistry, 2019, 91, 6141-6148.	6.5	24
130	A miniaturized UV-LED photochemical vapor generator for atomic fluorescence spectrometric determination of trace selenium. Journal of Analytical Atomic Spectrometry, 2018, 33, 1217-1223.	3.0	22
131	Cadmium and cobalt ions enhanced-photochemical vapor generation for determination of trace rhenium by ICP-MS. Applied Spectroscopy Reviews, 2022, 57, 318-337.	6.7	22
132	Methanol-Enhanced Liquid Electrode Discharge Microplasma-Induced Vapor Generation of Hg, Cd, and Zn: The Possible Mechanism and Its Application. Analytical Chemistry, 2021, 93, 8257-8264.	6.5	22
133	Inductively coupled plasma mass spectrometry for determination of total urinary protein with CdTe quantum dots label. Journal of Analytical Atomic Spectrometry, 2011, 26, 2493.	3.0	21
134	Determination of ultratrace nitrogen in pure argon gas by dielectric barrier discharge-molecular emission spectrometry. Microchemical Journal, 2011, 99, 114-117.	4.5	21
135	Chemical vapor generation from an ionic liquid using a solid reductant: determination of Hg, As and Sb by atomic fluorescence spectrometry. Journal of Analytical Atomic Spectrometry, 2016, 31, 415-422.	3.0	21
136	Sub-ppt determination of butyltins, methylmercury and inorganic mercury in natural waters by dynamic headspace in-tube extraction and GC-ICPMS detection. Journal of Analytical Atomic Spectrometry, 2017, 32, 2447-2454.	3.0	21
137	Headspace Solid-Phase Microextraction Following Chemical Vapor Generation for Ultrasensitive, Matrix Effect-Free Detection of Nitrite by Microplasma Optical Emission Spectrometry. Analytical Chemistry, 2021, 93, 6972-6979.	6.5	21
138	Photochemical Vapor Generation of Halides in Organic-Acid-Free Media: Mechanism Study and Analysis of Water Samples. Analytical Chemistry, 2021, 93, 11151-11158.	6.5	21
139	Determination of trace mercury in geological samples by direct slurry sampling cold vapor generation atomic absorption spectrometry. Mikrochimica Acta, 2008, 160, 191-195.	5.0	20
140	An optical humidity sensor based on CdTe nanocrystals modified porous silicon. Microchemical Journal, 2013, 108, 100-105.	4.5	20
141	Photochemical vapor generation for removing nickel impurities from carbon nanotubes and its real-time monitoring by atomic fluorescence spectrometry. Microchemical Journal, 2014, 117, 83-88.	4.5	20
142	UV-assisted Fenton digestion of rice for the determination of trace cadmium by hydride generation atomic fluorescence spectrometry. Analyst, The, 2016, 141, 1512-1518.	3.5	20
143	Amplified binding-induced homogeneous assay through catalytic cycling of analyte for ultrasensitive protein detection. Chemical Communications, 2016, 52, 1816-1819.	4.1	20
144	Spatially Constrained DNA Nanomachines To Accelerate Kinetics in Response to External Input: Design and Bioanalysis. Analytical Chemistry, 2020, 92, 8909-8916.	6.5	20

#	Article	IF	CITATIONS
145	Simple fluorescence sensing of extreme acidity based on inner filter effect of ascorbic acid to fluorescent Au nanoclusters. Nanoscale, 2017, 9, 10167-10172.	5.6	19
146	Synergy of adsorption and photosensitization of graphene oxide for improved removal of organic pollutants. RSC Advances, 2017, 7, 16204-16209.	3.6	19
147	Low-Temperature and Atmospheric Pressure Sample Digestion Using Dielectric Barrier Discharge. Analytical Chemistry, 2018, 90, 1547-1553.	6.5	19
148	Atomic spectrometry and atomic mass spectrometry in bioanalytical chemistry. Applied Spectroscopy Reviews, 2019, 54, 180-203.	6.7	19
149	A brief review on mass/optical spectrometry for imaging analysis of biological samples. Applied Spectroscopy Reviews, 2019, 54, 57-85.	6.7	19
150	Surface-enhanced Raman scattering using monolayer graphene-encapsulated Ag nanoparticles as a substrate for sensitive detection of 2,4,6-trinitrotoluene. Analytical Methods, 2017, 9, 3105-3113.	2.7	18
151	A silver nanoparticle-based colorimetric assay of trace selenium with hydride generation for sample introduction. Microchemical Journal, 2018, 141, 258-263.	4.5	18
152	Growth of Carbonaceous Nanoparticles on Steel Fiber from Candle Flame for the Long-Term Preservation of Ultratrace Mercury by Solid-Phase Microextraction. Analytical Chemistry, 2020, 92, 9583-9590.	6.5	18
153	Matrix-Assisted UV-Photochemical Vapor Generation for AFS Determination of Trace Mercury in Natural Water Samples: A Green Analytical Method. Spectroscopy Letters, 2010, 43, 550-554.	1.0	17
154	Effect of variable ultraviolet wavelength and intensity on photochemical vapor generation of trace selenium detected by atomic fluorescence spectrometry. Microchemical Journal, 2018, 140, 189-195.	4.5	17
155	Concentric DNA Amplifier That Streamlines In-Solution Biorecognition and On-Particle Biocatalysis. Analytical Chemistry, 2020, 92, 3220-3227.	6.5	17
156	Resurgence of Sandstorms Complicates China's Air Pollution Situation. Environmental Science & Technology, 2021, 55, 11467-11469.	10.0	17
157	Stimuli-Responsive Three-Dimensional DNA Nanomachines Engineered by Controlling Dynamic Interactions at Biomolecule-Nanoparticle Interfaces. ACS Nano, 2021, 15, 16870-16877.	14.6	17
158	Simultaneous Detection of Ruthenium and Osmium by Photochemical Vapor Generation-Inductively Coupled Plasma-Mass Spectrometry. Analytical Chemistry, 2022, 94, 593-599.	6.5	17
159	Application of Preconcentration and Separation Techniques in Atomic Fluorescence Spectrometry. Applied Spectroscopy Reviews, 2015, 50, 678-705.	6.7	16
160	A novel capillary microplasma analytical system: interface-free coupling of glow discharge optical emission spectrometry to capillary electrophoresis. Journal of Analytical Atomic Spectrometry, 2016, 31, 1423-1429.	3.0	16
161	Modification-free and N-acetyl-L-cysteine-induced colorimetric response of AuNPs: A mechanistic study and sensitive Hg2+ detection. Talanta, 2016, 159, 87-92.	5.5	16
162	Applications of silica-based nanoparticles for multimodal bioimaging. Applied Spectroscopy Reviews, 2018, 53, 377-394.	6.7	16

#	Article	IF	CITATIONS
163	Designing DNAzymeâ€Powered Nanomachines Simultaneously Responsive to Multiple MicroRNAs. Chemistry - A European Journal, 2018, 24, 19024-19031.	3.3	16
164	UV photochemical vapor generation–nitrogen microwave induced plasma optical emission spectrometric determination of nickel. Journal of Analytical Atomic Spectrometry, 2018, 33, 1086-1091.	3.0	16
165	Cross double point discharge as enhanced excitation source for highly sensitive determination of arsenic, mercury and lead by optical emission spectrometry. Journal of Analytical Atomic Spectrometry, 2021, 36, 1193-1200.	3.0	16
166	In-site and solvent-free exfoliation of porous graphene oxide from pencil lead fiber for solid-phase microextraction of cadmium ion before GF-AAS determination. Mikrochimica Acta, 2021, 188, 172.	5.0	16
167	Current advances of chemical vapor generation in non-tetrahydroborate media for analytical atomic spectrometry. TrAC - Trends in Analytical Chemistry, 2022, 155, 116677.	11.4	16
168	Inductively Coupled Plasma Optical Emission Spectrometry in the Vacuum Ultraviolet Region. Applied Spectroscopy Reviews, 2009, 44, 507-533.	6.7	15
169	A compact electrothermal-flame tandem atomizer for highly sensitive atomic fluorescence spectrometry. Journal of Analytical Atomic Spectrometry, 2012, 27, 1780.	3.0	15
170	In-atomizer atom trapping on gold nanoparticles for sensitive determination of mercury by flow injection cold vapor generation atomic absorption spectrometry. Journal of Analytical Atomic Spectrometry, 2014, 29, 367-373.	3.0	15
171	Ultrasensitive atomic fluorescence spectrometric detection of DNA with quantum dot-assemblies as signal amplification labels. Journal of Analytical Atomic Spectrometry, 2015, 30, 888-894.	3.0	15
172	Derivatization reaction-based surface-enhanced Raman scattering (SERS) for detection of trace acetone. Talanta, 2016, 155, 87-93.	5.5	15
173	Aggregation-induced phosphorescence enhancement of Mn-doped ZnS quantum dots: the role of dot-to-dot distance. Nanoscale, 2018, 10, 9236-9244.	5.6	15
174	Facile synthesis of chitosan membranes for visible-light-driven photocatalytic degradation of tetracycline hydrochloride. RSC Advances, 2020, 10, 45171-45179.	3.6	15
175	Simple Universal Strategy for Quantification of Carboxyl Groups on Carbon Nanomaterials: Carbon Dioxide Vapor Generation Coupled to Microplasma for Optical Emission Spectrometric Detection. Analytical Chemistry, 2020, 92, 3528-3534.	6.5	15
176	Molybdenum, Platinum, and Tantalum Metal Atomizers or Vaporizers in Analytical Atomic Spectrometry. Applied Spectroscopy Reviews, 2004, 39, 475-507.	6.7	14
177	Corona discharge radical emission spectroscopy: a multi-channel detector with nose-type function for discrimination analysis. Analyst, The, 2013, 138, 2249.	3.5	14
178	Dual-mode chemical vapor generation for simultaneous determination of hydride-forming and non-hydride-forming elements by atomic fluorescence spectrometry. Analyst, The, 2014, 139, 2538-2544.	3.5	14
179	In Situ Synthesis of Porous Carbons by Using Roomâ€Temperature, Atmosphericâ€Pressure Dielectric Barrier Discharge Plasma as Highâ€Performance Adsorbents for Solidâ€Phase Microextraction. Chemistry - A European Journal, 2015, 21, 13618-13624.	3.3	14
180	Reduction of mercury(II) by electrons contained in carbon dots: An environmentally friendly cold vapor generation for mercury analysis. Chinese Chemical Letters, 2020, 31, 2678-2682.	9.0	14

#	Article	IF	CITATIONS
181	Portable photochemical vapor generation-microwave plasma optical emission spectrometer. Journal of Analytical Atomic Spectrometry, 2020, 35, 1316-1319.	3.0	14
182	MnFe2O4 micromotors enhanced field digestion and solid phase extraction for on-site determination of arsenic in rice and water. Analytica Chimica Acta, 2021, 1156, 338354.	5.4	14
183	Improved hydride generation-atomic fluorescence spectrometry for determination of trace lead: minimization of blank from potassium ferricyanide. Analytical Methods, 2012, 4, 4058.	2.7	13
184	Mono-dispersed nano-hydroxyapatite based MRI probe with tetrahedral DNA nanostructures modification for inÂvitro tumor cell imaging. Analytica Chimica Acta, 2020, 1138, 141-149.	5.4	13
185	Novel "Turn-On―Luminescent Chemosensor for Arginine by Using a Lanthanide Metal–Organic Framework Photosensitizer. Analytical Chemistry, 2022, 94, 10271-10277.	6.5	13
186	Exploration of Displacement Reaction/Sorption Strategies in Spectrometric Analysis. Applied Spectroscopy Reviews, 2013, 48, 629-653.	6.7	12
187	Accelerating DNA nanomotor by branched DNAzyme for ultrasensitive optical detection of thrombin. Microchemical Journal, 2018, 139, 260-267.	4.5	12
188	Expanding DNA nanomachine functionality through binding-induced DNA output for application in clinical diagnosis. Chemical Communications, 2019, 55, 3610-3613.	4.1	12
189	Atmospheric low-temperature plasma for direct post-synthetic modification of UiO-66. Chemical Communications, 2020, 56, 5803-5806.	4.1	12
190	Visual detection of S ^{2â^'} with a paperâ€based fluorescence sensor coated with CdTe quantum dots via headspace sampling. Luminescence, 2021, 36, 1525-1530.	2.9	12
191	Ultrasensitive determination and non-chromatographic speciation of inorganic arsenic in foods and water by photochemical vapor generation-ICPMS using CdS/MIL-100(Fe) as adsorbent and photocatalyst. Food Chemistry, 2022, 375, 131841.	8.2	12
192	Improved Performance of On-line Atom Trapping in Flame Furnace Atomic Absorption Spectrometry by Chemical Vapor Generation: Determination of Cadmium in High-Salinity Water Samples. Spectroscopy Letters, 2009, 42, 240-245.	1.0	11
193	Direct Determination of Sodium Fluoride and Sodium Monofluorophosphate in Toothpaste by Quantitative ¹⁹ F-NMR: A Green Analytical Method. Spectroscopy Letters, 2009, 42, 334-340.	1.0	11
194	Dynamic reaction regulated surface-enhanced Raman scattering for detection of trace formaldehyde. Talanta, 2019, 202, 274-278.	5.5	11
195	A simple dilution method for the direct determination of trace nickel in crude oil with a miniaturized electrothermal atomic absorption spectrometer. Journal of Analytical Atomic Spectrometry, 2020, 35, 2656-2662.	3.0	11
196	Interface-free integration of electrothermal vaporizer and point discharge microplasma for miniaturized optical emission spectrometer. Analytica Chimica Acta, 2021, 1163, 338502.	5.4	11
197	Highly sensitive determination of trace antimony in water samples by cobalt ion enhanced photochemical vapor generation coupled with atomic fluorescence spectrometry or ICP-MS. Analytica Chimica Acta, 2022, 1191, 339361.	5.4	11
198	Mapping for total surface-enhanced Raman scattering to improve its quantification analysis. Talanta, 2016, 161, 151-156.	5.5	10

#	Article	IF	CITATIONS
199	On-line chemical vapor generation for determination of total sulfur dioxide in wine samples using an atomic fluorescence spectrometer. Journal of Analytical Atomic Spectrometry, 2018, 33, 161-167.	3.0	10
200	DNA-modulated photosensitization: current status and future aspects in biosensing and environmental monitoring. Analytical and Bioanalytical Chemistry, 2019, 411, 4415-4423.	3.7	9
201	Chemometric intraregional discrimination of Chinese liquors based on multi-element determination by ICP-MS and ICP-OES. Applied Spectroscopy Reviews, 2021, 56, 115-127.	6.7	9
202	Flow injection hydride generation and on-line W-coil trapping for electrothermal vaporization dielectric barrier discharge atomic emission spectrometric determination of trace cadmium. Talanta, 2021, 233, 122516.	5.5	9
203	A Compact Spectrophotometer Using Liquid Core Waveguide and Handheld Charge Coupled Device: For Green Method and Ultrasensitive Speciation Analysis of Cr(III) and Cr(VI). Spectroscopy Letters, 2009, 42, 351-355.	1.0	8
204	An oligonucleotide-based label-free fluorescent sensor: highly sensitive and selective detection of Hg2+ in aqueous samples. Analytical Methods, 2012, 4, 1310.	2.7	8
205	Selectively enhanced molecular emission spectra of benzene, toluene and xylene with nano-MnO ₂ in atmospheric ambient temperature dielectric barrier discharge. Analytical Methods, 2015, 7, 400-404.	2.7	8
206	Miniaturized point discharge-radical optical emission spectrometer: A multichannel optical detector for discriminant analysis of volatile organic sulfur compounds. Talanta, 2018, 188, 378-384.	5.5	8
207	Systematic Probing of the Sequence Selectivity of Exonuclease III with a Photosensitization Colorimetric Assay. ACS Omega, 2019, 4, 13382-13387.	3.5	8
208	Low Power, Low Temperature and Atmospheric Pressure Plasmaâ€Induced Polymerization: Facile Synthesis and Crystal Regulation of Covalent Organic Frameworks. Angewandte Chemie, 2021, 133, 10072-10077.	2.0	8
209	Miniaturized TOC analyzer using dielectric barrier discharge for catalytic oxidation vapor generation and point discharge optical emission spectrometry. Analytica Chimica Acta, 2021, 1172, 338683.	5.4	8
210	A miniaturized UV-LED array chip-based photochemical vapor generator coupled with a point discharge optical emission spectrometer for the determination of trace selenium. Journal of Analytical Atomic Spectrometry, 2021, 36, 2735-2743.	3.0	8
211	Dielectric barrier discharge-accelerated one-pot synthesis of sulfur quantum dots for fluorescent sensing of lead ions and <scp>l</scp> -cysteine. Chemical Communications, 2022, 58, 8614-8617.	4.1	8
212	L ysteine Enhanced Hydride Generation for Atomic Fluorescence Spectrometric Determination of Germanium in Geological Samples. Spectroscopy Letters, 2003, 36, 275-285.	1.0	7
213	Compact flame atomic absorption spectrometer based on handheld CCD for simultaneous determination of calcium and magnesium in water. Journal of Analytical Atomic Spectrometry, 2005, 20, 60.	3.0	7
214	Direct determination of deuterium of wide concentration range in water by Nuclear Magnetic Resonance. Talanta, 2012, 97, 450-455.	5.5	7
215	pH detection in biological samples by 1D and 2D 1H–31P NMR. Talanta, 2018, 178, 538-544.	5.5	7
216	Microplasma-induced vapor generation for rapid, sample preparation-free screening of mercury in fruits and vegetables. Analyst, The, 2021, 146, 3852-3857.	3.5	7

#	Article	IF	CITATIONS
217	UiO-66-NH2: An easily attainable and label-free turn-on probe for facile fluorescence sensing of alkaline phosphatase. Microchemical Journal, 2022, 179, 107516.	4.5	7
218	Online multichannel ultrasonic extraction for high throughput determination of arsenic in soil by sequential injection slurry hydride generation atomic fluorescence spectrometry. Analytical Methods, 2013, 5, 3142.	2.7	6
219	Point discharge microplasma reactor for high efficiency conversion of H2S to SO2 for speciation analysis of sulfide and sulfite using molecular fluorescence spectrometry. Analytica Chimica Acta, 2018, 1042, 79-85.	5.4	6
220	A signal conversion system using bindingâ€induced strand displacement for disease biomarker assay. Luminescence, 2021, 36, 1483-1490.	2.9	6
221	Microdischarge in Flame as a Source-in-Source for Boosted Excitation of Optical Emission of Chromium. Analytical Chemistry, 2022, 94, 7683-7691.	6.5	6
222	Exploration of nano-surface chemistry for spectral analysis. Science Bulletin, 2013, 58, 2017-2026.	1.7	5
223	Universal and label-free photosensitization colorimetric assays enabled by target-induced termini transformation of dsDNA resistant to Exo III digestion. Chemical Communications, 2019, 55, 7211-7214.	4.1	5
224	Determination of the isotopic composition of lutetium using MC-ICPMS. Analytical and Bioanalytical Chemistry, 2020, 412, 6257-6263.	3.7	5
225	Determination of the Isotopic Composition of Gadolinium Using Multicollector Inductively Coupled Plasma Mass Spectrometry. Analytical Chemistry, 2020, 92, 6103-6110.	6.5	5
226	A facile photochemical strategy for the synthesis of high-performance amorphous MoS ₂ nanoparticles. Nanoscale Advances, 2021, 3, 2830-2836.	4.6	5
227	<i>In situ</i> optical spectroscopy for monitoring plasma-assisted formation of lanthanide metal–organic frameworks. Chemical Communications, 2022, 58, 5419-5422.	4.1	5
228	Direct Current Arc Atomic Emission Detected by a Handheld Spectrometer Based on a Charge Coupled Device. Applied Spectroscopy Reviews, 2003, 38, 295-305.	6.7	4
229	Onâ€Line Spectrophotometric System Based on Pseudo Liquid Drop and Handheld CCD Spectrometer for Monitoring Formaldehyde Level in Wastewater. Instrumentation Science and Technology, 2005, 33, 297-307.	1.8	4
230	Saturated Solution of PbSO4as Standard Stock Solution and Its Applications in Analytical Spectroscopy: Screening Analysis of Lead in Natural Water andUsnea longissima. Spectroscopy Letters, 2007, 40, 537-545.	1.0	4
231	Building an anti-interfering DNAzyme-powered micromachine resistant to being inhibited by biological matrices. Chemical Communications, 2020, 56, 2658-2661.	4.1	4
232	Sensitive detection of trace 4-methylimidazole utilizing a derivatization reaction-based ratiometric surface-enhanced Raman scattering platform. Talanta, 2022, 237, 122925.	5.5	4
233	Nanoscale metal organic frameworks and their applications in disease diagnosis and therapy. Microchemical Journal, 2022, 180, 107595.	4.5	4
234	Modelling of catalytically oxidative decomposition of carbon tetrachloride on a ZnS nanocluster using density functional theory. Catalysis Science and Technology, 2014, 4, 1038.	4.1	3

#	Article	IF	CITATIONS
235	Toehold-regulated competitive assembly to accelerate the kinetics of graphene oxide-based biosensors. Journal of Materials Chemistry B, 2020, 8, 3683-3689.	5.8	3
236	Can low-temperature point discharge Be used as atomic emission source for sensitive determination of cyclic volatile methylsiloxanes?. Analytica Chimica Acta, 2020, 1124, 121-128.	5.4	2
237	Quantification of 13C, 15N labelled compounds with 13C, 15N edited 1H Nuclear Magnetic Resonance spectroscopy. Talanta, 2021, 224, 121839.	5.5	2
238	Activation of catalytic DNAzyme by bindingâ€induced DNA displacement for homogeneous assay. Luminescence, 2021, 36, 1498-1506.	2.9	2
239	An overview of alcoholic beverages discrimination and a study on identification of bland Chinese liquors by ¹³ C-NMR and ¹ H-NMR spectra. Applied Spectroscopy Reviews, 2023, 58, 252-270.	6.7	2
240	Proteinâ€Recognitionâ€Initiated Exponential Amplification Reaction (PRIEAR) and Its Application in Clinical Diagnosis. ChemBioChem, 2022, , .	2.6	2
241	Biomolecule-guided co-localization of intermolecular G-rich strands for the construction of a tetramolecular G-quadruplex sensing strategy. Chemical Communications, 2022, 58, 6914-6917.	4.1	1
242	Guest editor's introduction to the special issue on analytical spectrometry in China. Applied Spectroscopy Reviews, 2016, 51, 93-93.	6.7	0
243	Catalysts in photochemical vapor generation. , 2022, , 265-281.		0